Time-Resolved Fluorescence and FCS Studies of Dye-Doped DNA

N. Nicolaou, R. J. Marsh, T Blacker, D. A. Armoogum, and A. J. Bain*
Department of Physics & Astronomy, University College London, Gower Street, London WC1E 6BT

ABSTRACT

Fluorescence lifetime, anisotropy and intensity dependent single molecule fluorescence correlation spectroscopy (I-FCS) are used to investigate the mechanism of fluorescence saturation in a free and nucleotide bound fluorophore (NR6104) in an antioxidising ascorbate buffer. Nucleotide attachment does not appreciably affect the fluorescence lifetime of the probe and there is a decrease in the rate of intersystem crossing relative to that of triplet state deactivation. The triplet state fraction is seen to plateau at 72% (G-attached) and 80% (free fluorophore) in agreement with these observations. Measurements of translational diffusion times show no intensity dependence for excitation intensities between 1 and 10^5kW cm^{-2} and photo-bleaching is therefore negligible. The dominant mechanism of fluorescence saturation is thus triplet state formation. I-FCS measurements for Rhodamine 6G in water were compared with those in the ascorbate buffer. In water the triplet fraction was saturated at considerably higher powers (45% at ca. 1.5×10^3kW cm^{-2}) than in the ascorbate buffer (55%ca. 1 1kW cm^{-2}).

KEYWORDS

Fluorescence Lifetime, Fluorescence Correlation Spectroscopy, Single Molecule, Photo-bleaching

1. BACKGROUND AND CONTEXT

The demand for high throughput, low error, low cost automated DNA sequencing instrumentation has led to advances in dye based parallelized DNA sequencing methods [1]. Dye terminator sequencing is the method of choice in automated DNA sequencing techniques allowing for multiple sequencing in a single reaction by utilizing fluorescent chain terminating nucleotide analogues [2].To this end the development of high quantum yield and photostable fluorophores is essential. Fluorophores in which there is a marked probability once excited of singlet to triplet intersystem crossing exhibit long microsecond-millisecond times where the molecule is unable to absorb or emit radiation [3]. This trapping together with photobleaching [4] can prove a significant impediment to the successful implementation of this technology. In this context knowledge of a potential fluorophores photophysical pathways together with an assessment of its photostablility are a crucial starting point, as are the modification of its photophysical behavior by nucleotide incorporation. In this study we investigate the mechanisms of fluorescence saturation of a recently developed sequencing probe NR6104 (Illumina Cambridge Ltd) together with the fluorescent dynamics of Rhodamine 6G in both aqueous and oxygen scavenging environments.

The saturation of fluorescence from a molecular population can arise from a number of mechanisms. Under continuous wave excitation the relative decrease and the eventual saturation of the measured fluorescent count rate can arise from both increased trapping in dark (triplet) states and photobleaching, Such behavior is readily observed in NR6104 solutions as can be seen from figure 1 which shows the variation in fluorescence intensity of a micromolar solution of G-Nucleotide attached NR6104 under continuous wave excitation at 532nm in a confocal microscope (see section 3). In order to investigate the mechanisms responsible for this behavior we undertake time resolved fluorescence measurements of free (NR6104) and bound (G-NR6104) fluorophores. Investigation of triplet trapping and photobleaching bound and free NR6104 are undertaken using intensity dependent fluorescence correlation spectroscopy [5].

* corresponding author a.bain@ucl.ac.uk

Nanophotonic Materials VI, edited by Stefano Cabrini, Taleb Mokari, Proc. of SPIE Vol. 7393,
73930L · © 2009 SPIE · CCC code: 0277-786X/09/$18 · doi: 10.1117/12.826043

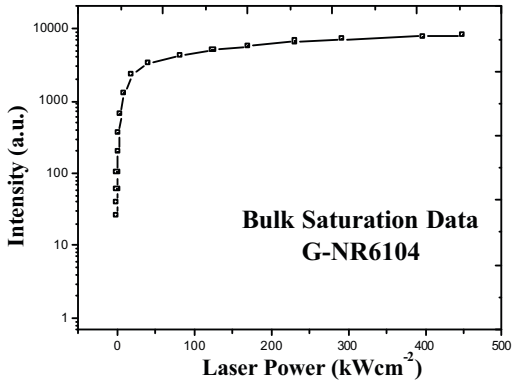

Figure 1: Saturation of a micromolar solution of G-NR6104 in ascorbate buffer. There is an approximately linear increase in fluorescence with excitation power (?=532nm) up to 20kWcm^{-2} with full saturation being evident at ca. 200kWcm^{-2}

2. TIME RESOLVED FLUORESCENCE STUDIES

Polarized time-resolved fluorescence experiments on free and bound NR6104 were undertaken using TCSPC. The apparatus and techniques used to obtain the fluorescence anisotropies and fluorescence lifetimes ('magic angle' detection) are described in detail elsewhere [6, 7]. Sample excitation (λ_{exc}=532nm) was achieved using the output of an Optical Parametric Oscillator (APE-Mira-OPO) synchronously pumped by a modelocked Ti:Sapphire oscillator (Mira-Coherent). Sample emission was isolated between 550-600nm using long pass (Schott OG550) and short pass (Corion LS600) filters. Decay analysis was performed using MicroCal™ Origin and PicoQuant Fluofit Software. The NR6104 samples were diluted (μM concentration range) in an ascorbate buffer and measurements were undertaken in 45μl^3 fluorescence cuvettes (Hellma UK) at room temperature (20±1°C). Fluorescence lifetime decays are shown in figure 2. Both DNA bound and free G-NR6104 exhibit biexponential fluorescence decays which are indicative of an inhomogeneous excited state population (e.g. different molecular conformations, emitting states etc).

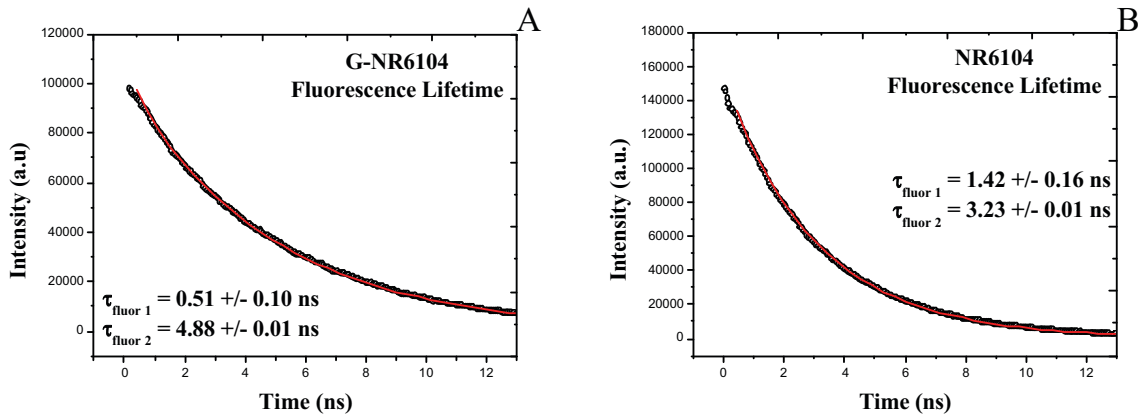

Figure 2: Fluorescence lifetime decays for G-NR6104 DNA bound (A) and free (B). Both exhibit two component decays, the average fluorescence lifetimes are 4.1 and 3.1ns respectively

Free NR6104 is characterized by two nanosecond lifetime components: with weighting 1.42ns (9%) and 3.32ns (91%). When bound to DNA a faster 510ps component (9%) and a slower 4.88ns component are observed (see figures 2A and 2B respectively) with no change in the weighting. These results are summarized in table 1. Attachment to the G-nucleotide results in longer lifetimes for both fast and slow components whilst their relative weights are unaffected. A reduction in fluorescence lifetime can result from quenching or an increased intersystem crossing rate (triplet formation), it is clear that nucleotide attachment does not lead to faster non-radiative relaxation of the fluorophore.

NR6104	$\tau_{fluor\ 1}$ (ns)	α_1(%)	$\tau_{fluor\ 2}$ (ns)	α_2(%)	χ^2
DNA Bound	0.51 +/- 0.10	9	4.88 +/- 0.01	91	2.31
Free	1.42 +/- 0.16	9	3.23 +/- 0.02	91	2.03

Table 1: Summary of the fluorescence lifetimes for free and DNA bound G-NR6104 (α is the proportion of each lifetime component (pre-exponential factor))

Fluorescence anisotropy measurements provide information on the local environment of a fluorescent probe and the overall rotational diffusion of the host/fluorescent probe system. Fluorescence anisotropy decay curves for the bound and unbound G-NR6104 in the ascorbate buffer are shown figure 3. NR6104 shows characteristic isotropic rotational diffusion with a 1.25ns decay time, comparable with diffusion of a small-medium sized fluorophore in a moderately viscous medium -the solution consisted of 1part tris buffer (NR6104 supplied in 100% tris buffer) to 10^4 parts ascorbate buffer. G-NR6104 in contrast shows a biexponential decay with a fast component of 610ps and a slow (overall) diffusion time of ca. 3ns. The 610ps component dominates the anisotropy decay (β_1= 0.32 vs β_2=0.02) characteristic of a loosely bound fluorophore (significant local orientational relaxation) attached to a more slowly diffusing structure. The anisotropy results are summarized in table 2

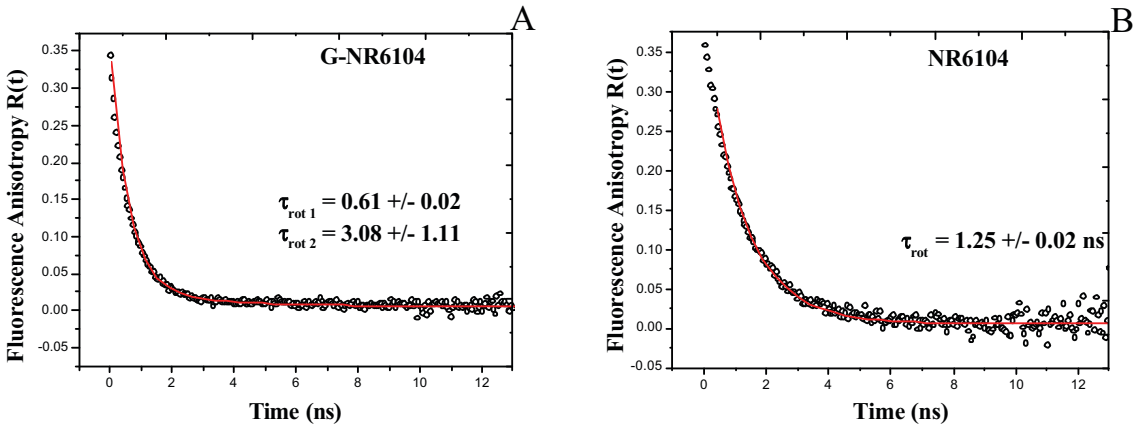

Figure 3: Fluorescence anisotropy decay curves for G-NR6104 DNA bound (A) and not bound (B). The fluorescence anisotropy decay of G-NR6104 bound to the DNA is not a single exponential and is best described with two correlation times. The anisotropy decay of unbound NR6104 is well described in terms of single exponential (isotropic) rotational diffusion

G-NR6104	τ_{rot1} (ns)	β_1	τ_{rot2} (ns)	β_2
DNA Bound	0.61 +/- 0.02	0.32	3.08 +/- 1.11	0.02
Free	1.25 +/- 0.02	0.37	-	-

Table 2 Fluorescence anisotropy data for bound and free G-NR6104, β_1 and β_2 are the relative weightings of the biexponential anisotropy decay

3 PHOTOBLEACHING AND TRIPLET FORMATION

3.1 Apparatus

Single molecule fluorescence correlation experiments were carried out using an inverted Olympus IX-71 microscope. The fluorescent samples (sub nM concentration) were placed over the microscope objective (Olympus UPlanSApo water immersion 60 x NA 1.2) where they were excited by the partial CW output of a diode pumped solid state laser (Coherent Verdi V10) at an excitation wavelength of 532nm. Sample fluorescence was separated following excitation via a dichroic mirror (Chroma Z535 RDC). Long pass (Semrock BLP01-532R-25) and short pass (Corion LS600) edge filters were used to isolate sample emission between 540-600nm and a confocal pinhole (50 μm) was used to isolate the focal plane. Fluorescence was detected by two silicon avalanche photo diodes (SPAD, Microphoton Devices SPCM-AQR-14) the output of which was sent to the TCSPC/FCS electronics (Picoquant PicoHarp) for analysis. The on sample power was measured using an ML9002A Anritsu power meter. A schematic of the experimental set-up is shown in figure 4

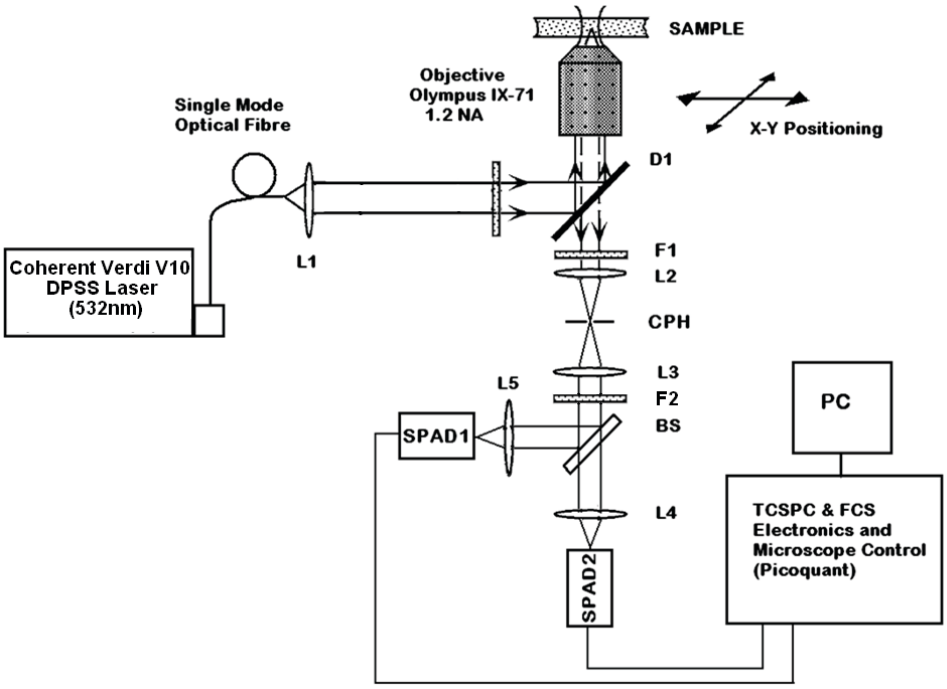

Figure 4: Schematic of the experimental set-up used to measure bulk saturation data. Fluorescence is detected using a confocal excitation-detection geometry yielding a sub femtolitre effective volume (0.276fl). L2 and L3 are confocal and collimating lenses; CPH the confocal pinhole (50μm); L4 and L5 SPAD focusing lenses; D1 a dichroic mirror (535nm long pass); F1 a 540nm long pass filter and F2 a 600nm short pass filter

3.2 Calibration of FCS Apparatus

FCS utilizes the temporal fluctuations in the fluorescence emission of small ensembles of molecules in an open excitation volume (sub-femtolitre) that is defined by the confocal geometry of the microscope. The spontaneous fluctuations in the fluorescence signal represent physical parameters, which through analysis of the fluorescence fluctuation autocorrelation function (AC) $G^{(2)}(\tau)$, provide information on molecular dynamics in the sub-microsecond to millisecond second time range.

The slowest dynamic process to be resolved temporally in a system of mobile molecules is diffusion through the excitation volume. Diffusion in the presence of triplet state blinking (assuming the shape of the focal volume is approximated by a 3-D Gaussian profile) is described by equation 1 [8, 9]

$$G(\tau)=\left[1-T+T\exp^{\left(\frac{-\tau}{\tau_T}\right)}\right]\Bigg/ N\left(1+\frac{\tau}{\tau_D}\right)^{-1}\left(1+\frac{\tau\omega_0^{\,2}}{\tau_D z_0^{\,2}}\right)^{\frac{1}{2}} \quad [1]$$

where τ_T is the (excitation rate-dependent) time constant for the triplet growth (triplet growth time), N is the average number of molecules present, z_0 is the effective focal radius along the optical axis at $1/e^2$ intensity, τ_D is the correlation time for diffusing molecules to traverse the confocal volume and is connected to ω_0, the effective lateral focus at $1/e^2$ intensity by the diffusion coefficient D (equation [2]) [10]

$$\omega_0^{\,2}=4D\tau_D \quad [2]$$

T is the dark (triplet) fraction of molecules, given by [11-13]

$$T=\frac{k_{23}k_{12}}{k_{12}\left(k_{23}+k_{31}\right)+k_{31}\left(k_{21}+k_{23}\right)} \quad [3]$$

where k_{12} is the excitation rate, k_{21} the spontaneous (S_1 to S_0 decay rate), k_{23} is the intersystem crossing rate and k_{31} the triplet recovery rate. The triplet growth time is given by

$$\frac{1}{\tau_T}=k_{31}+\frac{k_{23}k_{12}}{k_{12}+k_{21}} \quad [4]$$

The values of z_0 and ω_0 can be extracted by fitting the autocorrelation data to equation [1] providing the value for the diffusion coefficient of the fluorescent sample is known [14].The effective volume is then calculated from the values found for z_0 and ω_0 as it is related to the lateral and axial dimensions by [15]

$$V_{eff}=\pi^{3/2}w_0^2 z_0 \quad [5]$$

The correlation time for a diffusing species is related to the translational diffusion coefficient D (equation 2). This coefficient is determined by the Einstein equation for translational diffusion for a given temperature T[16]:

$$D=\frac{k_B T}{6\pi\eta R_H} \quad [6]$$

where k_B is the Boltzmann constant, ? is the solvent viscosity and R_H is the hydrodynamic radius of the diffusing species. Determination of the diffusion coefficient in new solvents for a given molecule could be achieved by utilizing equation [6] where the ratio of diffusion coefficients is equal to the reciprocal ratio of solvent viscosities [17]. With a value for the viscosity of the ascorbate buffer determined from time resolved anisotropy measurements[18] it was possible to calculate the translational diffusion constant for R6G in the ascorbate buffer from equation [6] using published data for the translational diffusion constant of R6G in water ($280\,\mu m^2\,s^{-1}$)[19]

$$D_{buffer}^{R6G}=\frac{\eta_{water}^{R6G}}{\eta_{buffer}^{R6G}}D_{water}^{R6G}=\frac{1.002}{17.60}\times 280=15.94\,\mu m^2 s^{-1} \quad [7]$$

Calibration of the apparatus to allow quantitative FCS experiments to be performed was achieved by undertaking a series of FCS measurements of R6G in the ascorbate buffer. It should be noted that the uncertainty in the value of the parameters

extracted by fitting the AC curves is concentration dependent [14]. It was therefore necessary to undertake a series of concentration dependent FCS experiments to determine the optimum concentration for the solution. Autocorrelation curves were recorded over a range of nM concentrations. FCS experiments were carried out at low intensity (0.6-6.4 $kWcm^{-2}$) to avoid saturation and distortion of the effective volume. Fitting the autocorrelation curves (using equation [1]) with a fixed translational diffusion coefficient ($16 \mu m^2 s^{-1}$) across the intensity range returned values for the lateral and axial dimensions (ω_0, z_0) and the effective volume which was found to be 0.276 +/- 0.1fl

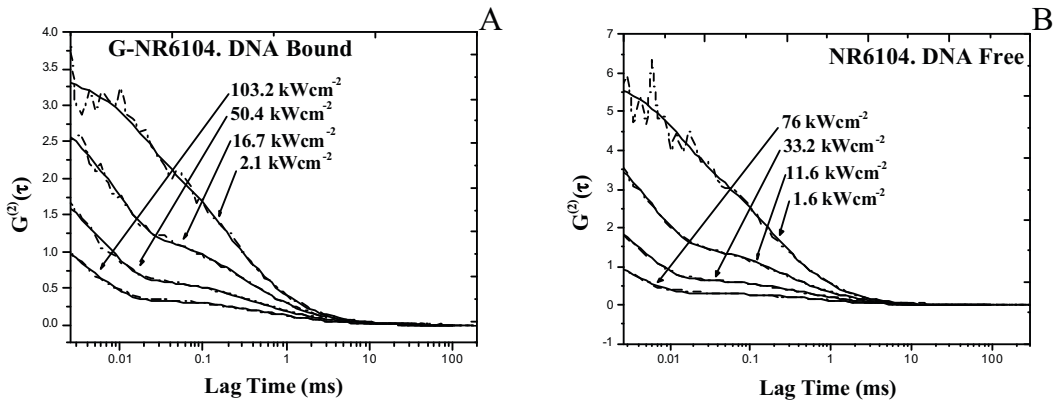

Figure 5: Experimental and fitted autocorrelation curves for bound (A) and free (B) G-NR6104 in ascorbate buffer at varying intensities. The amplitudes are not normalized.

The experimental autocorrelation curves for G-NR6104 bound (A) and free (B) are shown in figure 5.The autocorrelation curves are characterized by an increasingly pronounced fast time decay (µs range) component with increasing excitation intensity. This corresponds to the build up of a dark state (triplet) fraction as the probability of excitation to the singlet state and subsequent intersystem crossing to the triplet manifold rises. There is no noticeable shift in the long time tail region of the curve indicating that translational diffusion remains constant for both molecules. The variation in triplet fraction with excitation intensity is shown in figure 6A. It is apparent that there is an initial linear increase in the amount of triplet formed for bound and free G-NR6104, though for unbound NR6104 a lower power density is required to generate the equivalent triplet fraction -30% at 0.7 $kWcm^{-2}$ compared to a 21% fraction at 1.2 $kWcm^{-2}$ (bound). For free NR6104 the increase is linear to an excitation intensity of 6.7$kWcm^{-2}$ (ca. 60%) whereas for bound G-NR6104 the increase is linear to 4.6$kWcm^{-2}$ (ca. 42%). At higher power densities the rate of increase of triplet fraction for both bound and unbound decreases markedly. The triplet growth time is shown in figure 6B. Bound G-NR6104 displays a triplet growth time which is (on average) longer than free NR6104 (ca 15%) though there appears to be some convergence at higher power densities. The translational diffusion times are shown in figure 6C. These are similar and show little variation over the intensity range which is consistent with the form of the AC curves (ms range) in figures 5A and 5B.

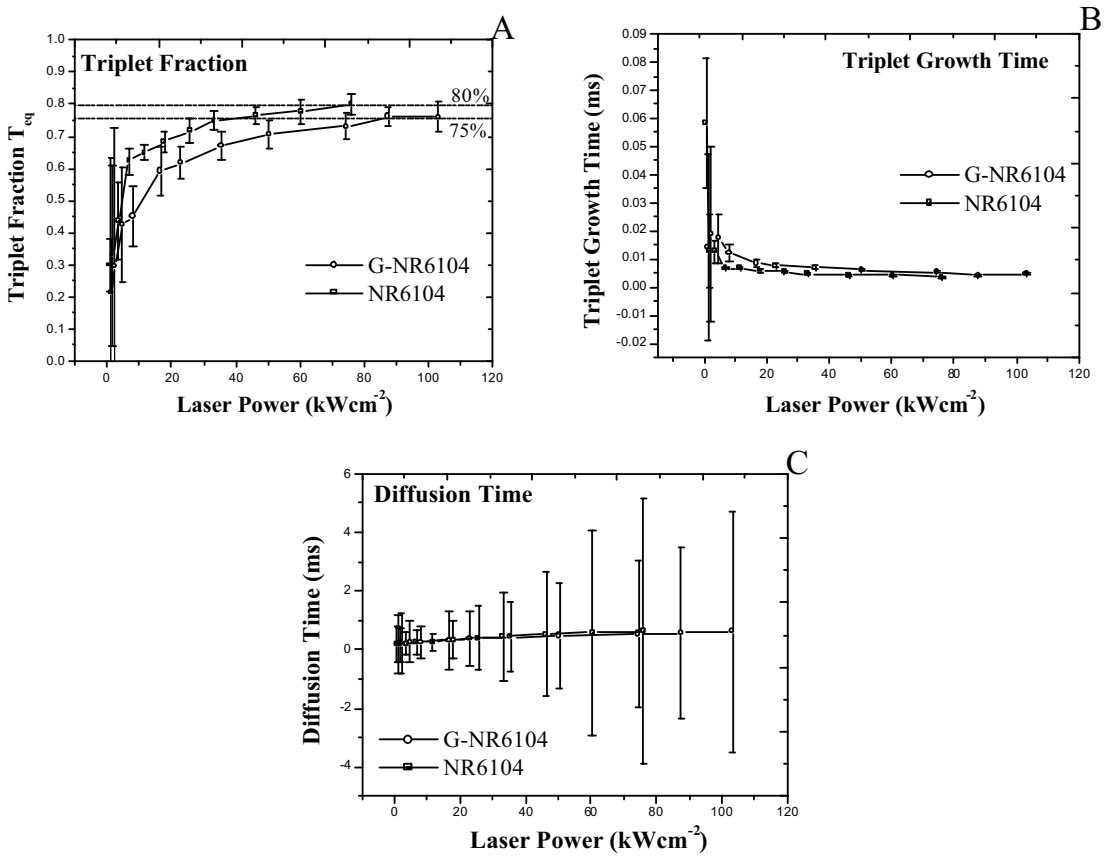

Figure 6: Dark (triplet) fraction (A), triplet fraction lifetime (B) and translational diffusion time (C) as a function of power density for the tagged and free NR6104

The relaxation pathways open to a fluorphore; intersystem crossing (rate k_{23}), triplet decay (rate k_{31}), excitation and de-excitation of the singlet state (rates k_{12} and k_{21}) are shown in figure 7. Vibrational relaxation following induced and spontaneous transitions within the singlet (S_0 and S_1) and triplet (T_1) manifolds is rapid (sub-picosecond) and can be considered to be effectively instantaneous compared to the intermanifold transition rates. Under these circumstances the population dynamics can be described in terms of a 3 level model [11, 12], from which the triplet fraction and triplet growth time (equation [1]) are given by

$$T = \frac{k_{23}k_{12}}{k_{12}(k_{23}+k_{31})+k_{31}(k_{21}+k_{23})} \quad [8]$$

$$\frac{1}{\tau_T} = k_{31} + \frac{k_{23}k_{12}}{k_{12}+k_{21}} \quad [9]$$

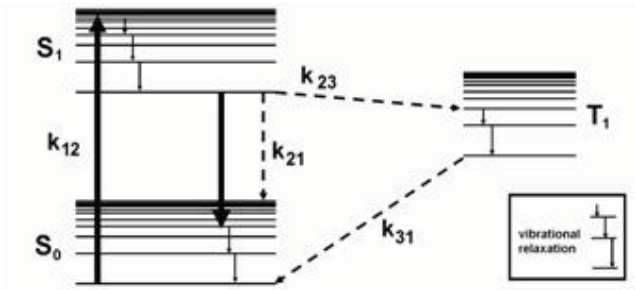

Figure 7: Jablonski diagram showing typical relaxation pathways open to an excited fluorophore

Simultaneous fitting of the T and τ_T data obtained from the FCS autocorrelation curves to equations [8] and [9] is shown in figure 8. Taking the excitation rate to be proportional to the excitation intensity ***I,***

$$k_{12} = AI \qquad [10]$$

this yields the ratio k_{23}/k_{31} and A for each fluorophore, these results are shown in table 4. It is evident from the values extracted for k_{23} and k_{31} that the ratio of intersystem crossing rate to triplet relaxation rate is greater for bound G-NR6104 (3.98) than for free NR6104 (3.36). The time dependence of the excited state population in a 3-level system has been derived elsewhere[12].

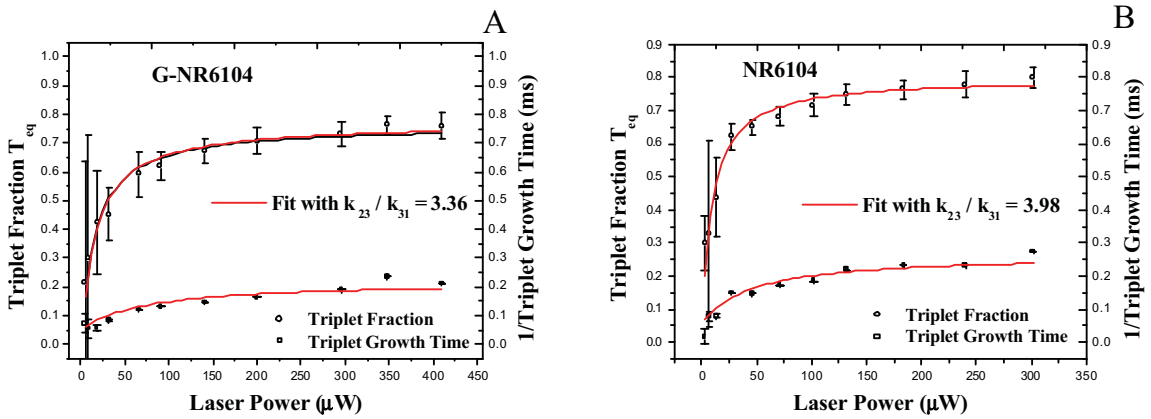

Figure 8: Triplet fraction change with power density for bound G-NR6104 (A) and free NR6104 (B). Fitting the data to equations 3 and 4 (assuming a linear power dependence of k_{12}) yields the ratio of the intersystem crossing rate k_{23} and triplet relaxation rate k_{31}

G-NR6104	Bound	Free
A	3.40	7.38
k_{23}/k_{31}	3.36	3.98

Table 5: Excitation Parameter A and ratio of the rate constants for bound G-NR6104 and free NR6104

It is clear from figure 8 that a lower saturated triplet fraction is produced in G-NR6104 (ca.70% vs. 80%), a similar ratio exists between the ratios of intersystem crossing to triplet relaxation rates (k_{23} / k_{31}) in the two molecules (table 5). These observations are consistent with the fluorescence lifetime measurements which indicate that removal of the G-nucleotide leads to a shorter fluorescence lifetime and hence faster non-radiative excited state relaxation. From figure 6C it can be seen that the diffusion time for both fluorophores remains constant (ca 500μs) with incident laser intensity indicating that up to 100kWcm^{-2} there is negligible photobleaching in NR6104. The lack of photobleaching together with the production of significant triplet fractions at high excitation powers implies that the saturation of fluorescence in G-NR6104 arises wholly from triplet state trapping. This can be modeled using the steady state limit of the three level model in which the fraction of the total population residing in the excited state (NE) is given by [12]

$$NE = \frac{Ak_{31}I\tau_f}{k_{31} + Ak_{23}I\tau_f + Ak_{31}I\tau_f} \qquad [11]$$

Here I is the excitation power and A is a coefficient proportional to the absorption cross section. Substituting values obtained above from fitting equations [3] and [4] into equation [13] produces the energy dependence of the excited state population shown in figure 9A. The saturation data extracted from the FCS measurements is shown in figure 9B.

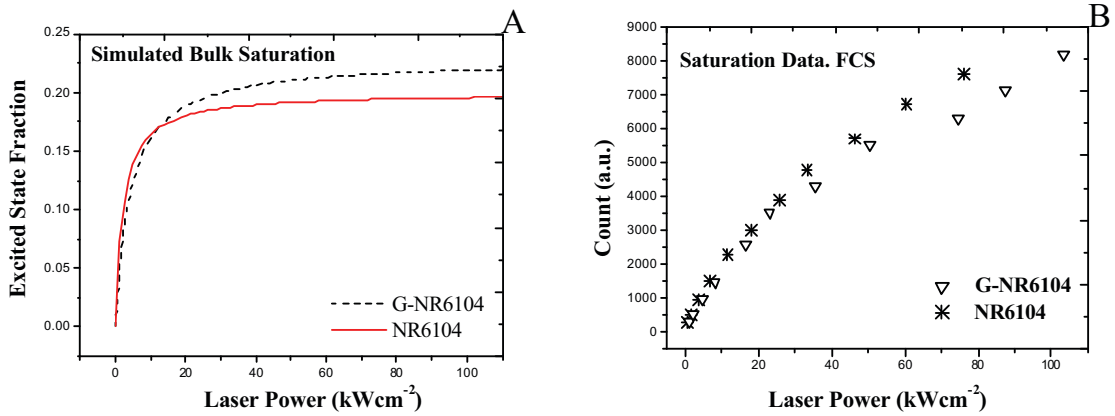

Figure 9: Simulated bulk saturation behavior for free and bound G-NR6104 (A) based on values extracted for the rate constants from figure 3.5 and (B) saturation data extracted from FCS measurements.

Figure 9A shows similar saturation behaviour to that of figure 1 and predicts that NR6104, whilst saturating at similar laser intensities to GNR6104, will give a lower fluorescence count. The low intensity data obtained from FCS intensity measurements (figure 9B) is consistent with a higher absorption cross section for the free fluorophore as in table 5.

4 FCS MEASUREMENTS OF RHODAMINE 6G IN WATER AND ASCORBATE BUFFER

The experimental set up for FCS measurements of Rhodamine 6G in water and in the ascorbate buffer are as described above. The experimental and fitted autocorrelation curves for R6G in ascorbate buffer (A) and R6G in water (B) recovered from the experiments are shown in figure 10.

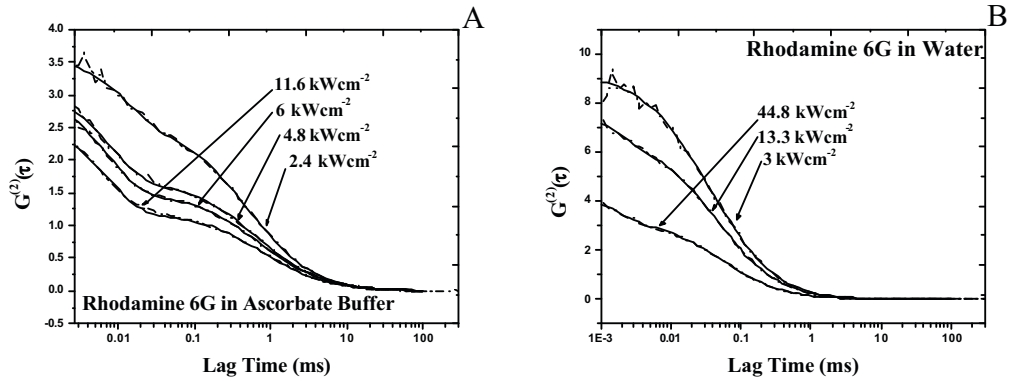

Figure 10: Experimental and fitted autocorrelation curves for R6G in ascorbate buffer (A) and R6G in water (B) at varying intensities. The amplitudes are not normalized

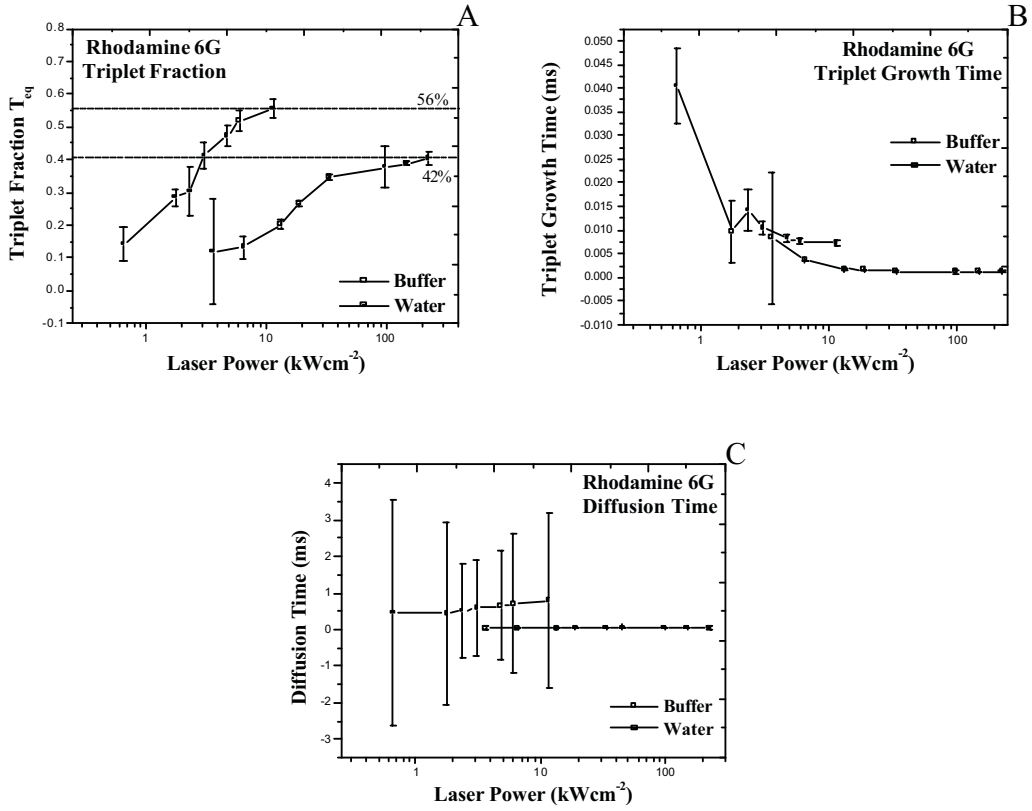

Figure 11: Triplet fraction (A), triplet growth time (B) and diffusion time (C) versus excitation intensity for Rhodamine6G in ascorbate buffer and Rhodamine6G in water.

The autocorrelation curves in the ascorbate buffer are characterized by an increasingly pronounced fast time decay component with rising excitation intensity, corresponding to the increasing probability of a molecule becoming trapped in the triplet manifold. The corresponding build up of the triplet fraction in water is far less pronounced. As with G-NR6104 there is no noticeable shift in the long time tail region of either FCS curve. The change in triplet fraction (A), triplet growth time (B) and diffusion time (C) with increasing excitation intensity is shown in figure 11. In the ascorbate buffer much less power is required to saturate the triplet fraction ca. 56% at 11kWcm^{-2} compared to ca. 42% at 1.5x10^{3} kWcm^{-2} in water. The diffusion times are shown in graph C and are independent of laser intensity.
Ascorbate buffers have been used as oxygen scavenging agents in single molecule fluorescence in order to reduce photobleaching [8,20] , our measurements indicate that in Rhodamine 6G, this leads to a larger triplet fraction, there is no discernable photobleaching in either solvent.

CONCLUSIONS

Saturation in GNR6104 and NR6104 does not occur as a result of photobleaching. This is evident from the constant translational diffusion time recorded for both constructs and from the lack of shortening of the diffusive tail of the FCS autocorrelation curves. Binding of the probe to the nucleotide does not appreciably affect the fluorescence lifetime though the fluorescence anisotropy for bound .G-NR6104 does exhibit a bi-exponential decay in contrast to the single exponential decay recovered for free NR6104. Detailed analysis of the FCS data yields photophysical parameters which (qualitatively) reproduce the form of the bulk saturation data for DNA bound G-NR6104. The triplet fraction is seen to saturate at ca. 80% for free and 75% for bound G-NR6104. The use of oxygen scavenging agents such as ascorbate, ostensibly to increase photostability, leads to enhanced triplet production which is the dominant mechanism for fluorescence saturation in freely diffusing single molecules.

ACKNOWLEDGEMENTS

We are grateful to EPSRC for financial support for this work.

8. REFERENCES

[1] Shendure, J., Ji, H., "Next Generation DNA Sequencing" Nat. Biotech. 26, 10 (2008)
[2] Guo, J., Xu, N., Li, Z., Zhang, S., Wu, J., Hyun Kim, D., Marma, M. S. Meng, O., Cao, H., Li, X., Shi, S., Yu, L., Kalachikov, S., Russo J.J., Turro, N.J., Ju, J., "Four-Color DNA Sequencing With 3_-O-Modified Nucleotide Reversible Terminators and Chemically Cleavable Fluorescent Dideoxynucleotides" PNAS. 105. (27). 9145–9150 (2008)
[3] Widengren, J., Rigler,R., "Mechanisms of Photobleaching Investigated by Fluorescence Correlation Spectroscopy" Bioimaging 4. 149-157. (1996)
[4] Eggeling C., Widengren, J., Rigler, R., Siedel, C.A.M., "Photobleaching of Fluorescent Dyes under Conditions Used for Single Molecule Detection: Evidence of Two Step Photolysis" Anal. Chem. 70 (13) (1998)
[5]Krichevsky O., Bonnet, G., "Fluorescence Correlation Spectroscopy: The Technique and its Applications" Rep. Prog. Phys. 65. 251-297. (2002)
[6] D V O'Connor and D V Phillips, "Time Correlated Single Photon Counting" Academic Press (1984)
[7] Marsh, R., Armoogum, D., Bain, A.J., J. Chem. Phys. Lett. 366. 398-405. (2002)
[8] Dittrich, P. S. and Schwille, P., "Photobleaching and stabilization of fluorophores used for single-molecule analysis with one- and two-photon excitation," App. Phys. B 73 829-837 (2001).
[9] Schwille, P., Kummer, S., Heikal, A. A., Moerner, W. E. and Webb, W. W., "Fluorescence Correlation Spectroscopy Reveals Fast Optical Excitation-Driven Intramolecular Dynamics of Yellow Fluorescent Proteins", Proc. Nat. Acad. Sci. U.S.A. 97, 151-156 (2000).
[10] Magde, D., Elson, E. L. and Webb, W. W., "Fluorescence Correlation Spectroscopy. II. An Experimental Realisation", Biopolymers 13 (1), 29-61 (1974).
[11] Widengren, J., Rigler, R. Mets, U., "Triplet-State Monitoring by Fluorescence Correlation Spectroscopy", J. Fluorescence 4, 255-258 (1994).

[12] Widengren, J., Mets, U. and Rigler, R., "Fluorescence Correlation Spectroscopy of Triplet States in solution: a theoretical and experimental study", J. Phys. Chem. 99, 13368-13379 (1995).

[13] Widengren, J., Mets, U. and Rigler, R., "Photodynamic properties of green fluorescent proteins investigated by fluorescence correlation spectroscopy", Chem. Phys. 250, 171-186 (1999).

[14] Buschmann, V., Kramer, B., Koberling, F., Macdonald, R., Ruttinger, S., "Quantative FCS, Determination of the Confocal Volume by FCS and Bead Scanning with the Microtime 200" Application Note.

[15] Krichevsky, O. and Bonnet, G., "Fluorescence Correlation Spectroscopy: the technique and its applications", Rep. Prog. Phys. 65, 251-297 (2002)

[16] Cang, H., Jie, L., and Fayer, M. D., "Orientational Dynamics of t he Ionic Organic Liquid 1-Ethyl-3-Methylimidazolium Nitrate", J. Chem. Phys. 119, (24) (2003)

[17] Armoogum, D.A., Marsh, R.J., Nicolaou, N., Mongin, O., Blanchard-Desce, M., Bain, A.J. "Stimulated Emission Depletion and Fluorescence Correlation Spectroscopy of a Branched Quadrupolar Chromophore" PROC. SPIE. 7020 (2008)

[18] Porter G, Sdakowski P J, Tredwell C J., "Picosecond Rotational Diffusion in Kinteic and Steady State Fluorescence", Chem. Phys. Lett. 49. 3. (1977)

[19] Visser, N. V., Hink, M. A., van Hoek, A. and Visser, A. J. W. G., "Comparison Between Fluorescence Correlation Spectroscopy and Time-Resolved Fluorescence Anisotropy as Illustrated with a Fluorescent Dextran Conjugate", J. Fluorescence 9 (3), 251-255 (1999).

[20] Aitken, C.E., Marshall, R.A. and Puglisi, J.D., " An oxygen scavenging system for the improvement of dye stability in single molecule fluorescence experiments" Biophys J. 94, 1826-1835 (2008)